Journal of Materials Chemistry A

Accepted Manuscript

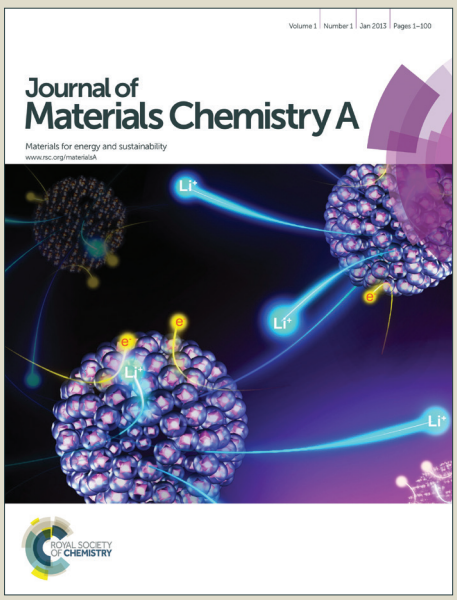

ROYAL SOCIETY OF CHEMISTRY

www.rsc.org/materialsA

Journal Name

RSCPublishing

ARTICLE

Surfactant recovery from mesoporous metal-modified materials (Sn-, Y-, Ce-, Si-MCM-41), by ultrasound assisted ion-exchange extraction and its re-use for a microwave in-situ cheap and eco-friendly MCM-41 synthesis

Cite this: DOI: 10.1039/xoxxoooooox

Received ooth December 2013,
Accepted ooth Xxxxx 2014

DOI: 10.1039/xoxxoooooox

www.rsc.org/

J. González-Rivera,[a] J. Tovar-Rodríguez,[a] E. Bramanti,[b] C. Duce,[c] I. Longo[d], E. Fratini,[e] I.R. Galindo-Esquivel[a] and C. Ferrari*[d]

Different metal substituted (Y, Sn and Ce) MCM-41 materials were synthesized and detemplated by a low temperature surfactant removal methodology. All metal substituted materials showed an increment in the d_{100} lattice parameter compared to the parent MCM-41 matrices. The increase depends on both the metal type and amount that is successfully incorporated by direct conventional hydrothermal synthesis. The metal modified MCM-41 materials were detemplated by an ultrasound assisted (US) ion-exchange process using methanol as solvent (NH_4NO_3/US/MeOH). The effect of ultrasound amplitude, extraction time and salt concentration were explored, and optimal values were determined for Y-MCM-41 detemplation (40 mM of NH_4NO_3, 60% of US amplitude and 15 min of adiabatic treatment). The removal percentage achieved with these values was in the following order: Y (97.7%) > Ce (94.4%) > Sn (92.1%) > Si (90.3%). Several techniques (SAXS, FTIR, TGA, ^{1}H MAS, ^{29}Si HPDEC MAS NMR and N_2 physisorption) demonstrated that the mesoporous materials keep their hexagonal structure and high surface area after the NH_4NO_3/US/MeOH surfactant extraction. Moreover, the thermal shrinkage of the structure was reduced in the following order: Si (0.6%) < Sn (4%) < Ce (5%) < Y (9%) < calcined samples (from 9 to 15%). The surfactant recovered was successfully recycled in a consecutive microwave assisted hydrothermal synthesis cycle (MW-HT). The synergy of different strategies (MW-HT synthesis, NH_4NO_3/US/MeOH surfactant removal and surfactant recovery) produces considerable time, energy and cost abatement, environmental impact reduction and promising scale up projections in the eco-friendly synthesis of MCM-41 materials.

1 Introduction

Recently, the use of MCM-41 mesoporous materials has been increasing in different applications such as catalysis[1] or heavy metal pollutant adsorbents in environmental applications.[1-3] They show unique properties, like high specific surface area, controllable pore size and well ordered hexagonal structure.[4]

The synthesis of siliceous MCM-41 has been widely studied and different methodologies have been proposed.[2-4] To modulate its surface properties, Si-MCM-41 can be modified with an active phase like metals[5,6] or enzymes[7-8] in post-synthesis treatments. On the other hand, direct insertion of different metals into the siliceous framework is typically done by the addition of the metal precursor in the synthesis gel followed by the hydrothermal crystallization process. Several metals have been tested for this purpose.[9-12]

The MCM-41 structure is build up by the presence of a structure directing agent, typically the surfactant molecule cetyltrimethylammonium bromide (CTAB). After the crystallization process, usually done at mild hydrothermal conditions, the CTAB must be removed from the inorganic structure to generate porosity. Calcination is generally used to remove the surfactant from the mesoporous structure. The process is carried out at high temperature under controlled conditions to avoid thermal shrinkage and structure damage. The conventional calcination process is highly undesirable since it might cause not only structure damage but it also presents high energy demands, requires long processing time and produces toxic residual pollution, which results in an increase of the catalysts production cost.

As alternative to the high temperature calcination process, several methodologies have been developed to remove the surfactant from the MCM-41 structure.[13-14] Two main approaches have been explored: 1) low temperature degradation and, 2) removal by solvent extraction. The first approach requires an oxidative system to degrade the surfactant, achieved by dielectric barrier discharge plasma,[15] H_2O_2,[16] microwaves[17] and Fe/H_2O_2.[18] Regarding the second approach, removal of the template has been achieved using acids[16,19] ammonium salts,[19,20] ultrasound[21] or supercritical CO_2 in alcoholic solvents.[22]

While both approaches are performed at low temperature levels, solvent extraction process seems more appealing since it opens the possibility to recover and further re-use the surfactant in the synthesis process. This is a very important fact from an economical point of view since about 50% w/w of the total quantity of MCM-41 synthesized corresponds to the surfactant molecule. Thus, the direct cost reduction in raw materials is clearly advantageous compared to the surfactant loss and pollution generation caused by its degradation.

The surfactant removal by extraction using alcohols seems to be the best approach, whereas some drawbacks still have to be solved. The mechanism could be a disruption of the surfactant aggregates caused by the organic solvent contact. Then, the non aggregated surfactant molecules are released to the solvent and easily elute from the mesopores. However, using solely organic solvents like ethanol does not allow the surfactant to be removed completely and some acids or cation exchangers have to be added to the extraction mixture. HCl in ethanol has been reported by some authors[16,19] and high detemplation was achieved. Nonetheless, the use of acids with alcohols can cause an esterification of the silanol groups in the MCM-41 surface and consequently, undesired changes in the material properties can occur.[19]

Considering the cationic nature of the surfactant CTAB, a solvent extraction using a similar salt cation producing an ion exchange between the dissolvent salt ions and the CTAB molecule anchored to the O_3SiO^- groups in the MCM-41 structure, is already well established. In particular, the pure silicon MCM-41 matrices were difficult to detemplate completely using NH_4NO_3 in ethanol and 3 cycles of 15 min were necessary.[20] However, it was also shown that an increment in the isomorphic metal (aluminium) substituted, resulted in higher surfactant removal, because CTAB molecules attached to O_3MO^- such as the tetrahedral aluminium atoms $[AlO_4]^-$ are easier to detemplate.

Following the mechanism of surfactant aggregates disruption, recently, Jabariyan and Zanjanchi[21] reported an efficient surfactant removal from Si-MCM-41 structure using low frequency ultrasound (US) irradiation in ethanol without any salt added. This approach still required more than one cycle to completely remove the surfactant from the mesopores.

The US assisted ion exchange methanol extraction of the surfactant from metal modified MCM-41 has not been explored so far. The synergy caused by the US irradiation and the ion-exchange salt is expected to increase the surfactant removal in a single cycle. In such a case, total removal of the CTAB could be easily achieved, causing a direct minimization of solvent use, energy consumption and processing time. Furthermore, this approach allows the CTAB to be recovered and re-used after a simple solvent distillation.

As mentioned above, both the diminution of total stages in the synthesis process of the metal modified MCM-41 and the reduction in pollution and final cost of the materials are desirable. In consequence, to develop an eco-friendly synthesis of metal modified MCM-41 mesoporous structures, direct incorporation of different metals (yttrium, tin and cerium) in the hydrothermal synthesis and a fast low temperature removal of surfactant from these structures are explored in this work. Furthermore, the possibility of an accelerated synthesis by microwave assistance has been explored, resulting in a considerable reduction of the synthesis time.

The effect of ultrasound amplitude, extraction time and salt concentration were studied in the low temperature ultrasound assisted ion exchange process (named as NH_4NO_3/US/MeOH surfactant extraction here on) and optimal values were determined for high detemplation. The recycling of the recovered surfactant has been demonstrated. Additionally, different conditions of the surfactant degradation by oxidative systems were compared.

The synergy of using different strategies like microwave assisted hydrothermal synthesis (MW-HT), low temperature NH_4NO_3/US/MeOH surfactant extraction and the recovery/re-use of surfactant and solvent resulted in a considerable time, raw material, energy, cost and environmental impact reduction in the synthesis of metal-MCM-41.

2 Results and discussion,

2.1 Characterization of M-MCM-41 synthesized mesoporous materials

Several well ordered metal modified MCM-41 structures were synthesized by hydrothermal crystallization process. Three different metal substituted (Y, Sn and Ce) materials were prepared. For comparative purposes, the chemical composition obtained by energy dispersed X-ray spectroscopy microanalysis (EDS) of the different materials is shown in Table 1 (see columns Si and M).

The nominal metal concentration for each material was selected considering the disparity between the tetrahedral silicon Si^{4+} and the ionic radius for the isomorphic substituted heteroatom. The ionic radius size decreases in the order Ce^{4+} (1.01 Å) > Y^{3+} (0.93 Å) > Sn^{4+} (0.71 Å) > Si^{4+} (0.41 Å) thus, the direct incorporation is expected to be difficult. Nevertheless, all the metals were successfully incorporated in the framework and, as expected, the poorest metal substitution occurred when the cerium incorporation was made. As the Ce^{4+} ionic radius is more than twice the size of Si^{4+}, only a third of the nominal metal loading was substituted. The Si/Ce ratio obtained was 153 compared to the nominal value of 50 (Table

1, columns A and B). The highest metal substitution was achieved for the Sn-MCM-41 material.

Table 1. Composition of as-synthesized metal modified MCM-41 materials by EDS analysis and lattice parameters.

Material	Si (w/w)	M(w/w)	Si/M		d_{100}, nm	a_0, nm
			A	B		
Si-MCM-41	100.0	---	---	---	4.77	5.5
Y-MCM-41	36.68	1.03	225	133	4.79	5.5
Sn-MCM-41	35.1	1.4	125	107	5.08	5.9
Ce-MCM-41	32.10	0.60	50	153	4.85	5.6

[A] nominal molar ratio Si/M; [B] calculated by microanalysis results

Figure 1a shows the Small Angle X-ray Scattering (SAXS) patterns for the synthesized MCM-41 materials. All the materials prepared exhibit four main diffraction peaks that can be indexed to the (*100*), (*110*), (*200*) and (*210*) planes associated to the hexagonal crystal system,[23] space group *p6mm*. For the parent Si-MCM-41 material (see Figure 1a), the (*hkl*) values assigned to the first three planes are found around the scattering vector (q) values of 0.15, 0.27 and 0.31 A^{-1} respectively. The spacing for the hexagonal lattice (Table 1, column d_{100}) was calculated by interpolation using these reflections. The unit cell a_0 constant (Table 1, column a_0) was calculated using Bragg's Law. Assuming that the nominal metal concentration was effectively incorporated, the d_{100} increase should follow the order Ce > Y > Sn. However, the d_{100} parameter increases depending on both, the size of the metal and the actual amount of heteroatom substituted. Given that Sn exhibits the highest quantity of metal incorporated successfully, the d_{100} increase was observed as Sn > Ce > Y. Since the chemical bonding Si-O-M is longer than the bonding Si-O-Si, the d_{100} spacing increment is in agreement with an incorporation of the metal in the framework. As the metal load increases, the diffraction peaks tend to shift to lower *q* values, which represent an increase in the unit cell parameters. A lower structural change is produced when Y is introduced in the structure. For this material, the small diffraction peak at 0.24 A^{-1} is consistent with the presence of a lamellar structure given by the surfactant. The most considerable effect is evident when Sn is incorporated in the MCM-41 structure, with a (100) diffraction peak displacement to q = 0.14 A^{-1}, indicative of a d_{100} value of 5.08 nm. Similar results have been reported for several metal modified MCM-41.[10,19] Regardless of the metal substituted, the hexagonal structure is well preserved for all materials.

2.2 Ultrasound assisted-NH_4NO_3/Methanol ion exchange extraction surfactant removal

A low temperature methodology for surfactant removal from the metal modified mesoporous MCM-41 synthesized structures was investigated. This methodology considered the use of ultrasound irradiation coupled with a low concentration ammonium salt solution in methanol.

While ethanol is the most widely used solvent for extraction, methanol has considerable advantages such as a lower boiling point (10 °C below that of ethanol) which allows a considerable energy saving in the solvent recovery process. Moreover, the solubility of CTAB in methanol is higher than the solubility when ethanol is used as solvent (greater than 0.75 M against 0.5 M in ethanol). The use of ultrasound further increases the solubility of CTAB, since the energy transferred to the solution increases the temperature. At 40 °C the solubility of CTAB in methanol increases beyond 1M.

Many other monovalent salts can be used as ion exchange agents. Different characteristic must be considered to increase surfactant removal efficiency while the structural surface properties remain unchanged. The ion exchange process can be described as a reversible chemical reaction wherein a ionic specie in solution (NH_4^+ for our system) is exchanged by a similarly charged ion ($(C_{16}H_{33})N^+(CH_3)_3$) attached to a fixed molecule in MCM-41 particles ($(O_3SiO^-$ or O_3MO^- groups). Thus, different and smaller counterions could cause different results due to ion exchange efficiency. In principle, the smallest counterion (as Na^+) could be more effective due to an easier access to the exchange sites. However, in our particular case, the use of ultrasound greatly increases the dynamics of the exchange process, so the counterion size should not be a critical parameter.

Furthermore, samples that had been extracted with alkali metal salts ($EtOH/NaNO_3$) presented: i) lower surface area; ii) lower mesopore volume than samples that had been extracted with either pure solvents or with acid-containing solutions, iii) are very unstable toward the following calcination step, and iv) show no catalytic activity (in Friedel–Crafts acylation of 2-methoxynaphthalene) demonstrating that active sites of the catalyst might be modified by the presence of sodium ions.[19,20]

The use of ammonium nitrate is the most logical choice, given that the calcined materials are usually ion exchanged in NH_4NO_3 solution to remove the residual sodium ions, and Brønsted acidity is created by heating the ammonium form.[19] Even more, the use of ammonium nitrate causes a weak interaction of the ammonium ions with the different groups on the surface on the MCM-41,[20] resulting in an easy condensation to produce the silanol or the active sites. This characteristic is very desirable for the final application of the synthesized materials.

The effect of three different factors (salt concentration, ultrasound amplitude and time) on a solvent extraction approach was investigated. The evaluation of the detemplation degree was done using FT-IR and TGA.

It seems that the disruption of micelles and the CTAB release to the methanol was fast, due to the synergy caused by the ultrasound energy and the high ion exchange efficiency of NH_4NO_3 in methanol. Thus, only one cycle of treatment is enough to achive high percentages of removal. Table 2 shows the results of the Y-MCM-41 detemplation for all the Box-Behnken experimental design runs. High detemplation values were achieved (99.3%, run 11, Table 2) after only one cycle of treatment. According to the analysis of variance (ANOVA), the

salt concentration (x_1) showed the main effect on the NH_4NO_3/US/MeOH surfactant extraction. Low concentration caused low removal whereas high concentration showed a negative effect, indicating that an optimal value should exist in the explored range.

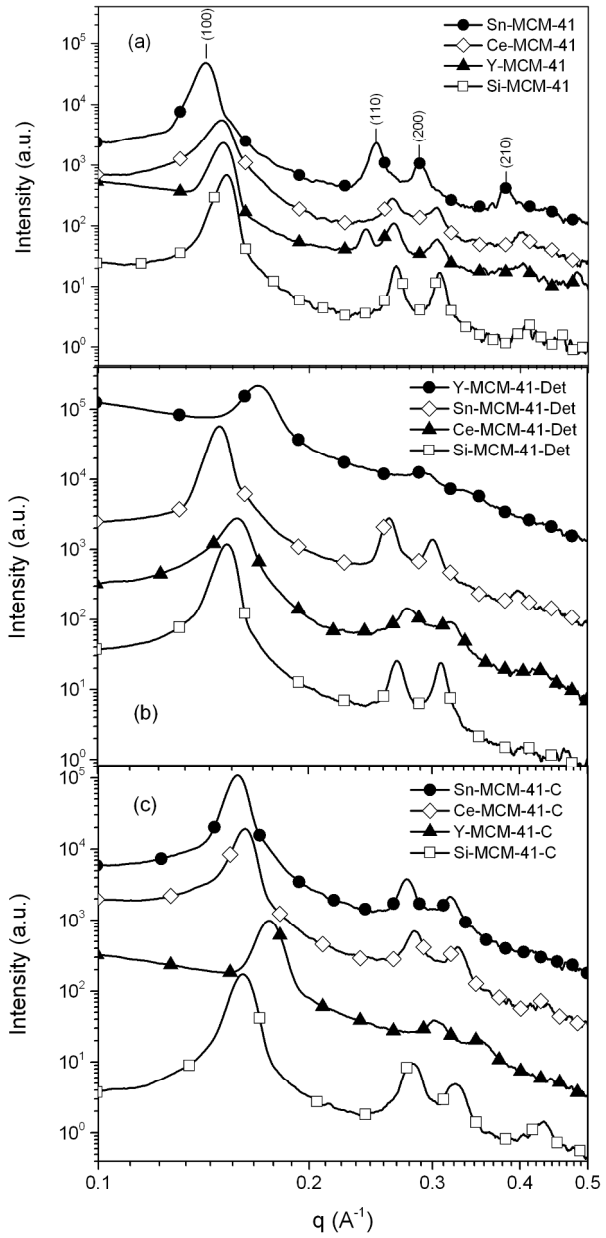

Figure 1. SAXS patterns: (a) materials containing the templating agent; (b) materials after NH_4NO_3/US/MeOH surfactant extraction under optimal conditions; (c) calcined samples.

The time (x_3) and the ultrasound amplitude (x_2) did not show considerable effect by themselves. However, the interaction between the US and NH_4NO_3 concentration contributed with positive effects. From the Box-Behnken surface response analysis, the optimal levels to maximize the surfactant removal were identified as: $x_1 = 0.6$, $x_2 = 1$, $x_3 = 1$. According to Table 6, the decoded values are: 40 mM of NH_4NO_3, 60% of US amplitude and 15 min of adiabatic treatment (the maximum temperature observed was below 50 °C and it depends on the different combination of the factors and its levels). These conditions were applied to the Sn-MCM-41, Ce-MCM-41 and Si-MCM-41 materials. The removal percentage achieved after the NH_4NO_3/US/MeOH surfactant extraction was in the order: Y > Ce > Sn > Si, with the corresponding values of 97.7, 94.4, 92.1 and 90.3%.

Table 2. Full experimental values of the Box-Behnken design

Run	x_1	x_2	x_3	Total area[A]	% removal[B]
1	-1	-1	0	11.9	69.2
2	0	+1	-1	1.2	96.9
3	+1	-1	0	1.9	95.1
4	+1	0	-1	2.3	94.1
5	0	0	0	2.1	94.5
6	-1	+1	0	14.3	63.1
7	0	-1	+1	1.7	95.7
8	-1	0	-1	14.5	62.4
9	0	-1	-1	2.0	94.9
10	+1	+1	0	0.9	97.8
11	+1	0	+1	0.3	99.3
12	0	0	0	1.9	95.1
13	0	0	0	2.0	94.9
14	0	+1	+1	0.5	98.8
15	-1	0	+1	12.0	68.9

[A] Calculated form integrated area of FTIR spectra; [B] calculated using the as-synthesized Y-MCM-41 FTIR area as 100%

Lang and Tuel[20] proposed a surfactant removing approach from aluminium modified and pure silica based MCM-41, using 250 mM of NH_4NO_3 at 60 °C in ethanol. They proposed that the surfactant removal percentage depends on the metal concentration, being greater for higher metal concentrations. In this work, the salt concentration was reduced to 40 mM (around 6 times less compared to the literature[20]) for high silica/Y molar ratio samples and full detemplation was achieved. This reduction can be due to the synergy between the cavitation effect produced by the ultrasound irradiation and the salt concentration. The sudden formation of cavities in the solvent might be contributing to facilitate the transport of the NH_4NO_3 inside the MCM-41 channels, accelerating the ion-exchange process. Similarly, the use of ultrasound to detemplate MCM-41 was recently reported by Jabariyan and Zanjanchi.[21] They achieved a 93% of detemplation from Si-MCM-41 when it was treated for 15 min using ethanol or methanol as solvent and ultrasound. To fully remove the surfactant, they used more cycles under sonication. Their reported methodology was focused solely on pure siliceous MCM-41 and the metal modified materials were not explored.

2.3 Characterisation of M-MCM-41 NH_4NO_3/US/Methanol extracted mesoporous materials

Figure 2 shows the FTIR spectra for the materials containing the surfactant, after the low temperature removal and the calcined samples. Several bands are associated to the presence of the surfactant into the MCM-41 samples: i) the bands at 2924 and 2850 cm^{-1} correspond to the bending vibration (–C–

H) of the $–CH_2–$ and $–CH_3$ groups in the C_{16} aliphatic chain of the CTAB molecule, respectively; ii) the –C–H stretching vibration and alkylammonium vibration are assigned in the region of 1490 to 1380cm^{-1}; iii) a weak signal at 725 cm^{-1} is also assigned to the symmetrical vibration in the plane (rocking). For all the calcined samples, these bands are not present. After the NH_4NO_3/US/MeOH surfactant extraction, the peaks assigned to the hexadecyltrymethylammonium molecule are minimized or completely reduced.

The peak signals at around 1090, 970, and 465 cm^{-1} are assigned to the stretching and bending vibrations of silica-oxygen tetrahedrons. The NH_4NO_3/US/MeOH surfactant extraction produces no changes in these bands and after the treatment, these peaks remain unmodified. It is important to note that no signals were identified in the region from 1400 to 1450 cm^{-1} typically for NH_4^+ ions. This result suggests a weak interaction between this group and the modified metal or silanol groups (Si–OH) which tend to be reactive.

The FTIR and the SAXS analyses (Figures 1 and 2) demonstrate that the mesoporous materials keep their hexagonal structure without considerable changes after the NH_4NO_3/US/MeOH surfactant extraction. In the particular case of pure Si- and Sn- modified structures, the scattering patterns remains identical to the as-synthesized materials. Y- and Ce-MCM-41 samples show small reduction in the intensity of SAXS peaks. Both structures showed the greater response to the surfactant removal treatment and achieved the highest percentage removal. These results suggest that the modified metal has additional effects on the surfactant removal beyond the factors explored in the Box-Behnken analysis. Further optimization for each individual material should be done, to obtain the maximum surfactant removal.

Confirmatory experiments of the surfactant removal were carried out using thermo-gravimetric analysis. The temperature region of the surfactant removal was explored using FTIR spectroscopy coupled to TG analysis. The experiments were performed under air atmosphere to emulate the calcination process. In the case of the Y-MCM-41 and Sn-MCM-41, different mass loss regions were identified (see Figure 3): the first event was at temperatures below 120 °C corresponding to the physisorbed water into the mesopores. Then from 120 to 270 °C the CTAB was successfully removed. From 270 to 350 °C the TMAOH molecule was burned. The drop in mass after 350 °C was due to the water release produced by the silanol condensation and also the oxidation of the residual carbonaceous material after an incomplete surfactant and/or co-surfactant combustion. In the case of Ce-MCM-41 and Si-MCM-41 similar trend was observed, however the synthesis of these two materials did not involve the use of a co-surfactant molecule (TMAOH). The mass loss of surfactant in all cases was estimated in the temperature range of 120 to 350 °C. The results were in agreement with the FTIR quantitative analysis.

Table 3 summarizes the textural properties for the calcined and extracted materials. The pore diameter of the MCM-41 is typically in the range of 2 to 10 nm.[23] After the surfactant treatment (either calcination or NH_4NO_3/US/MeOH surfactant extraction), these materials exhibited a narrow pore size distribution from 2 to 4 nm (see Table 3, column D). The materials subject to high temperature surfactant removal showed large pore diameters. The modified metal caused an expected effect on the pore size: when cerium was introduced in the silica framework, a higher pore modification was produced, compared to the parent material composed of pure silica. In contrast, yttrium produced a lower pore size change, for both surfactant removal treatments (calcined and NH_4NO_3/US/MeOH surfactant extraction). A bimodal pore size distribution was shown by Y-MCM-41 (pore size of 2.2 and 3.2 nm) and Ce-MCM-41 (pore size of 2.4 and 4.0 nm). This bimodal pore size distribution can be attributed to the difference in ionic sizes of the modified metals. If the metal incorporation in the MCM-41 structure is inhomogeneous, the periodicity changes and results in pores with an increased size. This can be applied to Ce- and Y-MCM-41. However, Sn-MCM-41 showed only one pore size distribution suggesting high periodicity and homogeneous metal incorporation.

Table 3. Structural (SAXS) and textural parameters of mesoporous materials (Values between parentheses refer to extracted materials)

Material	S_{BET} (m^2/g)[a]	V (cm^3/g)[b]	D (nm)[c]	d (nm)[d]	a_0 (Å)[e]	W (Å)[f]
Y-MCM-41	1077	0.94	2.94	4.2	48	19
	(925)	(0.70)	(2.38)	(4.3)	(50)	(26)
Ce-MCM-41	806	0.77	3.83	4.2	48	10
	(870)	(0.64)	(2.77)	(4.6)	(53)	(25)
Sn-MCM-41	1129	1.03	3.63	4.6	53	17
	(955)	(0.88)	(2.43)	(4.9)	(56)	(32)
Si-MCM-41	1044	0.94	3.56	4.1	48	12
	(1023)	(0.82)	(2.75)	(4.7)	(55)	(27)

[a] BET specific surface area, [b] BJH pore volume, [c] BJH average pore diameter, [d] d interplanar spacing of the four reflections derived from the q-vector value, [e] hexagonal unit cell, [f] wall thickness as a_0-D.

The specific surface area was high in all cases (see Table 3, column S_{BET}). Ce-MCM-41 detemplated using NH_4NO_3/US/MeOH surfactant extraction shows a higher surface area than the calcined sample even though 5% of surfactant still remains in the framework. On the other hand, the Y-MCM-41 calcined sample exhibits a higher surface area than the fully surfactant removed sample by NH_4NO_3/US/MeOH surfactant extraction. In the case of Sn- and Si-MCM-41 materials, the specific surface area was higher for the calcined materials than for the extracted samples. For those materials, the remaining surfactant in the structures was about 8 and 10% respectively. The latest values can explain the difference in the value of S_{BET} in the case of Sn- and Si-MCM-4. It's possible to affirm that not only the surfactant removal contributes to increase the surface area value S_{BET}, but also the presence of the substituted metal in the framework had a significant effect, when compared with the Si-MCM-41.

Journal Name RSCPublishing

ARTICLE

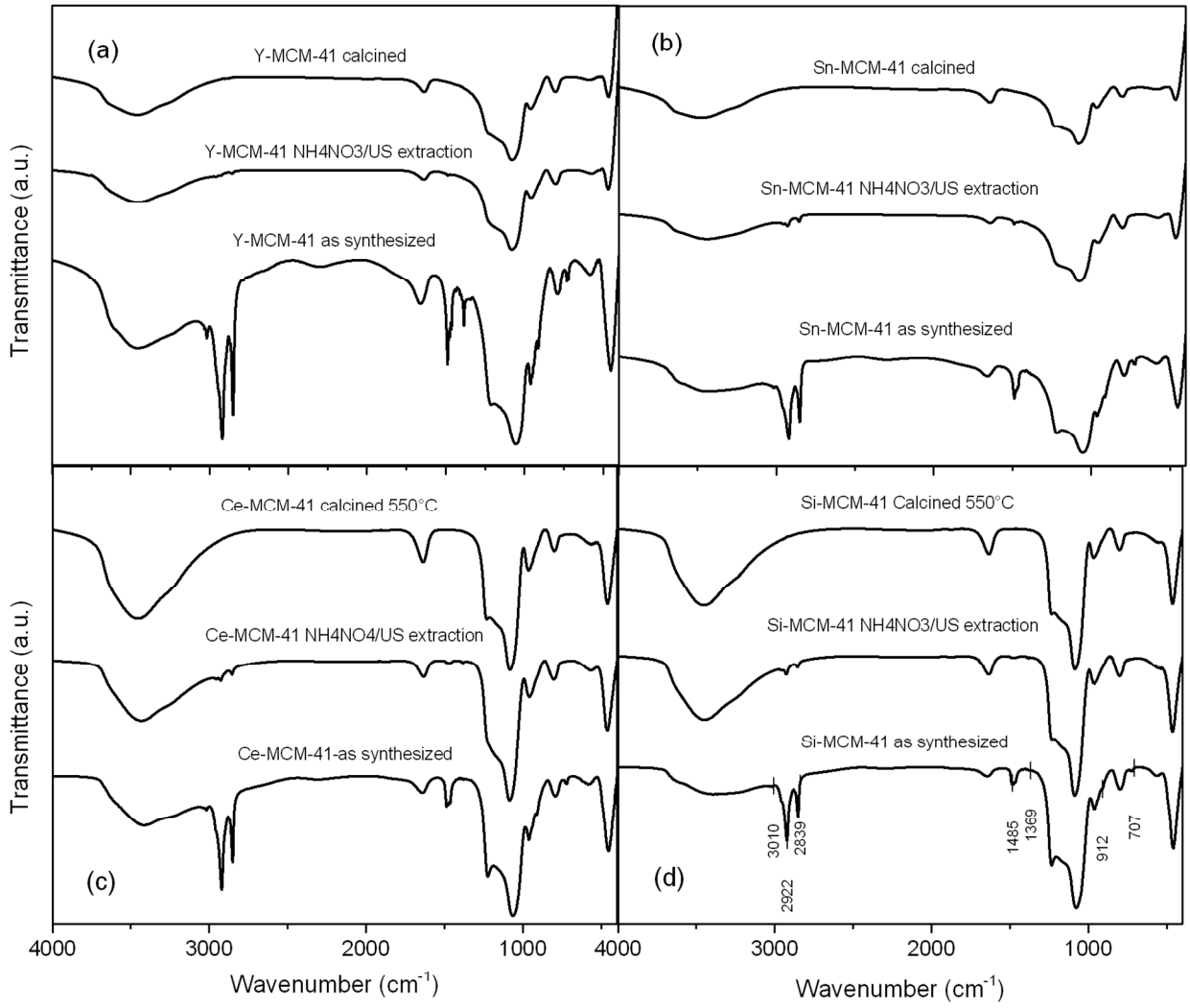

Figure 2. FTIR Spectra for: (a) Y-MCM-41; (b) Sn-MCM-41; (c) Ce-MCM-41 and (d) Si-MCM-41 after calcination, NH_4NO_3/US/MeOH extraction and as synthesized materials.

Journal Name RSCPublishing

ARTICLE

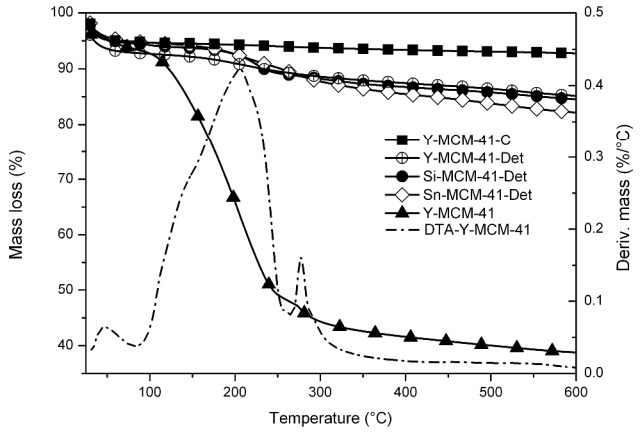

Figure 3. TG analysis for (Y-MCM-41) and extracted samples (Y, Si, Sn-MCM-41).

The structural parameters for the calcined and NH_4NO_3/US/MeOH surfactant extraction detemplated materials are also shown in Table 3. The cell unit value of all samples changes after both surfactant removal approaches (Table 3, column a_o). High temperature calcination can cause a framework contraction due to the dehydroxylation and siloxane bonds formation known as thermal shrinkage.[24] The thermal shrinkage can be referred as TS = 1-a_{02}/a_{01} where a_{02} and a_{01} are the cell unit value of the detemplated and as-synthesized materials respectively. For the calcination process, the TS calculated values ranged from 9 to 15%. The highest framework contraction was shown by Ce-MCM-41 and Si-MCM-41 and it was estimated to be 14%. Sn-MCM-41 showed 9% and 13% for the Y-MCM-41 material. The remaining surfactant in the frameworks did not affect the TS value, as mentioned elsewhere.[25]

On the other hand, after the low temperature NH_4NO_3/US/MeOH surfactant extraction proposed, the TS can be minimized to 0.6% in the case of Si-MCM-41. The metal modified structures showed lower TS values in the order of Y > Ce > Sn with 9, 5 and 4% respectively. In all cases, the values are smaller than the TS caused by calcination. In the case of the NH_4NO_3/US/MeOH surfactant extraction, the metal modified structures can experiment a unit cell reduction produced by the ion exchange mechanism, where the NH_4^+ interacts with the metal substituted (see Table 3, column a_0). The highest unit cell contraction was shown by Y-MCM-41. In this framework, after yttrium was incorporated in the silica network, it could be stabilized by NH_4^+ ions. However, from the spectroscopic characterization there is no evidence of ammonium groups linked to the framework, due to the absence of significant signals in the 1400 to 1450 cm^{-1} interval. This could indicate a structural rearrangement once the surfactant molecule is removed.

SEM micrographs for the metal modified extracted samples are shown in Figures 4a-c. Ce-MCM-41 shows the smaller particle size (around 0.5 μm) with predominant round ball shape morphology (see Figure 4a). In the case of Sn-MCM-41 (Figure 4b), a wide particle size distribution was observed (from 1 to 10 μm) with an irregular shape in the biggest particles to round ball shape morphology showed by the smallest particles. Y-MCM-41 shows worm-like to round ball shapes with a wide particle size distribution (see Figure 4c). The aggregation patterns depend on the different metal modified synthesized MCM-41 materials. Sn-MCM-41 showed less aggregation and well defined particles when compared with Ce- and Y-MCM-41.

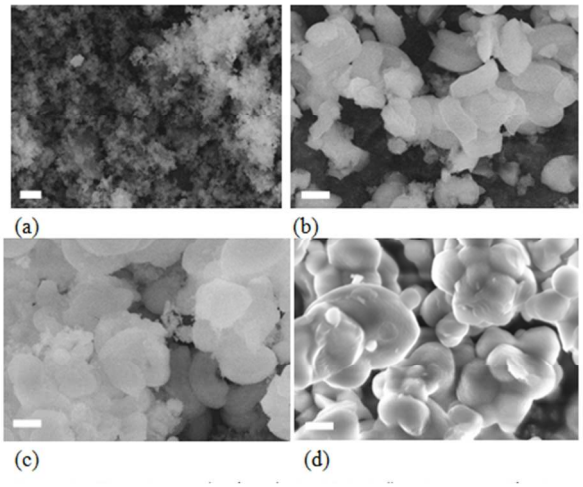

Figure 4. SEM micrographs for: a) Ce-MCM-41 (bar=4μm, magnification 5kX); b) Sn-MCM-41 (bar=4μm, magnification 5kX); c) Y-MCM-41 (bar=4μm, magnification 5kX) after the NH_4NO_3/US/MeOH surfactant extraction treatment and d) silica MCM-41 (bar=400nm, magnification 50kX) synthesized from surfactant recovered and re-used.

2.4 Effect of the metal concentration on the ion exchange extraction

In order to study the effect of the same metal concentration on the low temperature surfactant removal and possible structural changes, two new metal modified MCM-41 materials were synthesized: Sn- and Ce-MCM-41 were prepared with the same Si/Y ratio (Si/M = 225). For these materials, the removal percentage achieved after the NH_4NO_3/US/MeOH surfactant extraction was in the order: Y > Sn > Ce > Si, with the corresponding values of 97.7, 95.9, 93.6 and 90.3%. These

results show that at the same metal concentration, Y-MCM-41 still showed the highest surfactant removal whereas the surfactant percent removal changed considerably for Sn-MCM-41 (from 92.1 to 95.9%) when the tin concentration was reduced 2:1. In the case of the Ce-MCM-41 not significant effect was found (less than 1% of variation) when the Si/Ce ratio was changed from 50 to 225. It seems that the metal concentration (at least at the same nominal concentration) has an effect on the low temperature surfactant removal and it depends on the nature of the metal used to modify the Si-MCM-41 structure.

2.5 Solid State NMR characterization of the M-MCM-41 (Si/M = 225) mesoporous materials

Solid state nuclear magnetic resonance studies using magic-angle spinning (MAS NMR) have proven an important role in the structural characterization of some important solids such as the inorganic mesoporous MCM-41 materials[26] and the microporous zeolites.[27] A multinuclear analysis approach can lead to complement the structural characterization since ^{29}Si MAS NMR provides accurate information regarding the environment of silicon atoms both in the structure framework and present on the surface. Ultrafast ^{1}H MAS NMR gives valuable information about the surface groups and the water molecules bonded to the silanol groups through hydrogen bonds. Even more, indirect information can be obtained about the influence and the environment of the different metal isomorphycally substituted into the hexagonal structure. Other heteronucleous analysis such as ^{119}Sn MAS NMR and ^{89}Y MAS NMR can help to determine the metal coordination state and structural interaction in the analyzed solids. However, some technical limitations involve low sensitivity and low concentration of the metal into the solid materials. In these cases the physical determination by MAS NMR is sometimes not feasible.

The high power decoupling ^{29}Si MAS NMR spectra of the M-MCM-41 materials (Si/M = 225) after the low temperature surfactant removal and the calcined samples are compared with the as synthesized materials in Figure 5.

All calcined samples exhibit a broad band from -90 to -120 ppm with no distinctive peaks. The spectra for detemplated and as synthesized metrials show two distinctive peaks assigned to Q^3 and Q^4 environments at around -102 and -111 ppm values of chemical shift, which confirms that the proposed ion-exchange extraction methodology results in materials with similar Q^n distribution compared to the as synthesized materials.

In order to obtain the single Q^4, Q^3 and Q^2 values assigned to siloxane groups ($Si(O\text{-}Si)_4$), isolated silanol groups ($(\text{-}O\text{-})_3\text{-}Si\text{-}OH$), and germinal silanol groups ($(\text{-}O\text{-})_2\text{-}Si\text{-}(OH)_2$), the deconvolution of the spectra obtained between -80 and -120 ppm was performed. Table 4 presents the Q^n values after spectra deconvolution for calcined, NH_4NO_3/US/MeOH extracted and as synthesized metal modified MCM-41 materials, considering a Gaussian-Lorentzian ratio equal to 0.7 selected to better adjust the typical NMR signal. To compare the relative amount of silanol and siloxane in the samples, the isolated silanols/silaxane (Q^3/Q^4) and total silanol/siloxane ($(Q^2+Q^3)/Q^4$) ratios were calculated (Table 4, entries 5 and 6).

For the as synthesized metrials containing the same nominal amount of metal substituted, a change in the silicon coordination given by different distribution of Q^n groups is clearly observed. The type and coordination of the heteroatom incorporated produces a unique modification to the silicon environment, when compared to the pure siliceous MCM-41.

The calcination treatment to remove the surfactant molecules produces the highest loss of silanolic sites. At least half of the total silanol groups in the original material are condensed with the high temperature treatment to form siloxane bridges or totally eliminated to form water molecules. The surface siloxane bonds formed are hydrophobic and do not produce surface rehydration or water adsorption to favour the reverse process to regenerate the Si-OH sites.[28]

The NH_4NO_3/US/MeOH extraction approach produces silanolic sites loss to a lesser extent. For the Y-MCM-41, the silanol loss has a similar magnitude compared to the calcination procedure. For the rest of the materials, a lower silanol condensation allows the material to keep more active sites than their calcined counterparts. The two distinctive bands for Q^4 and Q^3 are kept (see Figure 5) and tend to be displaced to lower values of chemical shift, depending on the metal substituted, which proves to have a significant effect on the Q^n distribution as well as the surfactant removal treatment. While the calcination treatment causes a surface dehydroxilation, the proposed methodology to remove surfactant allows the materials to keep a significant amount of the original silanolic sites and may result in the design of specific materials with the desired hydrophobic or hydrophilic properties, since the surface characteristics could be tailored.

Table. 4 Q^n distribution for calcined, detemplated and as synthesized metal modified MCM-41 materials

Sample		Q^4	Q^3	Q^2	Q^3/Q^4	$(Q^2+Q^3)/Q^4$
Si- MCM-41	Calc.	50.37	38.41	9.65	0.76	0.95
	Det.	46.26	45.89	7.84	0.99	1.16
	As syn.	25.87	54.15	19.37	2.09	2.84
Sn-MCM-41	Calc.	55.79	40.95	3.25	0.73	0.79
	Det.	47.66	39.95	12.39	0.84	1.10
	As syn.	30.55	42.24	25.53	1.38	2.22
Y- MCM-41	Calc.	48.9	45.71	5.04	0.93	1.04
	Det.	50.74	40.72	8.08	0.80	0.96
	As syn.	28.04	67.03	4.93	2.39	2.57
Ce-MCM-41	Calc.	64.3	32.32	3.38	0.50	0.55
	Det.	48.1	47.24	4.66	0.98	1.08
	As syn.	36.51	27.72	34.56	0.76	1.71

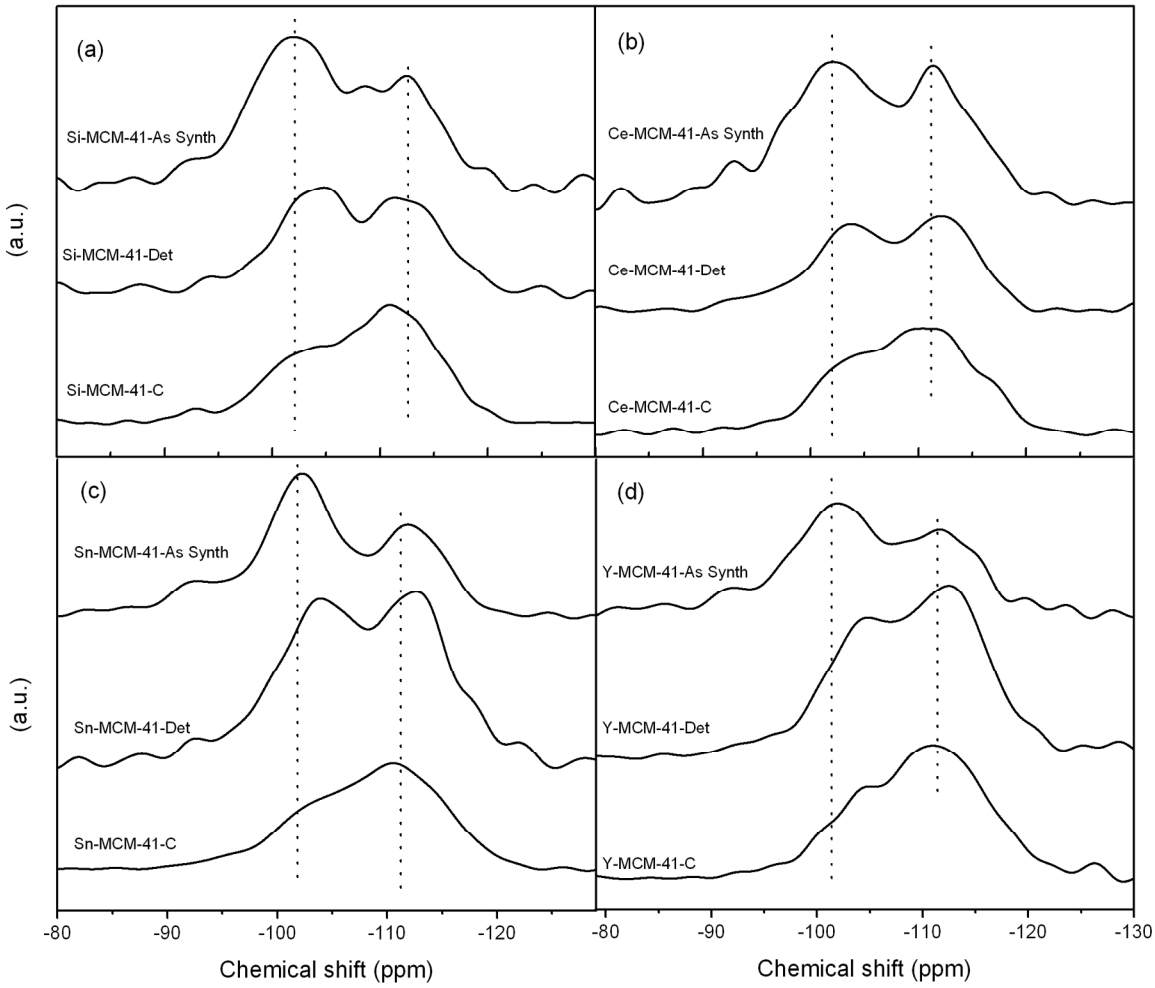

Figure 5. ^{29}Si HPDEC MAS NMR Spectra of the metal modified mesoporous materials: (a) Si-MCM-41, (b) Ce-MCM-41, (c) Sn-MCM-41 and (d) Y-MCM-41.

High-speed ^{1}H MAS (50 KHz) lead to a sensitive and simple approach for acquiring the high-resolution NMR spectra in MCM-41 samples. According to Tréboc et al[29] the CTAB molecule inside the mesopores of Si-MCM-41 shows three well-resolved peaks at 0.8, 1.2, and 3.1 ppm assigned to the -CH_3, -CH_2-, and -CH_2-N$(CH_3)_3$ protons in the surfactant molecules inside the mesopores. In the ^{1}H MAS NMR spectra, the surface groups of Si-MCM-41 (free isolated silanoles, -Si-OH, Q^3-like environments detected by ^{29}Si HPDEC MAS NMR) are typically assigned to the chemical shift value of 1.8 ppm for dried and degasified metrials. The presences of physisorbed water into the mesopores are well detected by the ^{1}H chemical shift of water molecules in hydrated samples of MCM-41. Grünberg, et al[30] mentioned three main water environmental sites for the siliceous MCM-41. When the water content in the mesoporous material is about 3 to 6%, the molecules tend to interact due to their high polarity by hydrogen-bonding with the hydration sites (-SiOH) on solid surface (-$Si_{surface}$-OH + H_2O ⟹ -$Si_{surface}$-OH:OH_2) and this signal can be detected about 2.5 ppm. Hydrogen bonded clusters of water molecules may begin to form as water molecules bond (at concentration bigger than 23%) to the previously adsorbed water ($Si_{surface}$-OH: OH_2+H_2O ⟹ $Si_{surface}$-$OH_2(OH_2)$ with a chemical shift around 4.7 ppm. Other weak signals for the free water molecules without any surface interaction (movil clusters) can appear in the whole range from 1 to 6 ppm.

The ^{1}H MAS NMR spectra for the as synthesized Ce-MCM-41 (Si/Ce = 225) containing the surfactant (CTAB), after the ion exchange extraction and the calcined sample are shown in Figure 6a. For all the metal modified MCM-41 as synthesized materials, three main chemical shifts around 4.5, 2.6 and 2.2 ppm can be identified. In the analyzed samples of this work, the chemical shifts at 2.2 and 2.6 ppm could be assigned to the CTAB molecule inside the pores of the as synthesized materials and the residual surfactant molecule for the incomplete detempleated M-MCM-41 materials since these chemical shifts decrease after the two treatments. Even more, the intensity reduction value is more evident for the calcined samples. However, since the analyzed samples did not receive previous treatment such as degasification or thermal heating to remove the physisorbed water, the chemical shift around 2.5

ppm can also be related to the water molecules bonded to the hydrated surface (-$Si_{surface}$-OH:OH_2), specially in the case of the calcined and the NH_4NO_3/US/MeOH extracted samples. The chemical shift around 4.5 ppm exhibited by the as synthesized materials can be assigned to the hydrogen bonded clusters of water molecules mentioned above. This chemical shift showed a displacement to lower ppm after the two treatments for the surfactant removal. In the case of the low temperature surfactant removal, it seems that the water–silanol configurations and associated proton chemical shifts are more complex than only a single hydrogen bonding mentioned before since at least three different peaks are apparently visible. However, a detailed investigation on these possible interactions is beyond the scope of this work. In the case of the calcined samples, a wide signal distributed from 3 to 5 ppm is related to the water-silanol and the mobile clusters mentioned elsewhere.[31]

Figure 6b shows an enlarged area of the ^{1}H MAS NMR spectra in the interval from 8 to 5 ppm. The spectra show a chemical shift at around 6.3 ppm which corresponds to the NH_4NO_3/US extracted samples. These chemical shifts were detected due to the bonding of ammonium ions after the ion exchange treatment and were not present for the as synthesized and calcined samples. As it is shown in Figure 6b, the peaks show a displacement from 6.3 to 6.1 ppm in the following order: Y > Sn > Ce. These chemical shifts displacement depend on the nature of the metal and it could be an indirect evidence of the isomorphic substitution of the metal into hexagonal siliceous MCM-41 framework. These ^{1}H MAS NMR results seem to indicate that the Y and Sn incorporation appear to generate more acidic sites than the rest of the materials, which is generally true when different coordination and electronegativity heteroatoms are substituted into the oxide structure.

2.6 Comparative study on Sn-MCM-41 detemplation by oxidative systems and NH_4NO_3/US/MeOH surfactant extraction

To compare the low temperature NH_4NO_3/US/MeOH surfactant extraction proposed in this work, several other surfactant degradation approaches using oxidative systems were applied to the metal modified Sn-MCM-41 synthesized mesoporous structure. The FTIR spectra for the different approaches listed in Table 5 are shown in Figure 7. The efficiency of each surfactant degradation method is reported in Table 5.

The effectiveness in the surfactant degradation using a photochemical reactor and different combination of the oxidative agents was low in all cases. Several reports indicate that the use of high contact time and oxidative agent concentration is effective to achieve high detemplation at mild conditions.[18] In this work, 60 min and low concentration of oxidative agents were explored. Moreover, the combination of different oxidative agents and the simultaneous irradiation of microwaves and UV energy did not improve the efficiency of degradation in the contact time selected. The main drawback of all these treatments was the loss of the surfactant molecule.

Table 5. Surfactant removal efficiency by oxidative and solvent extraction applied to Sn-MCM-41

System	Time (min)	Temperature (°C)	% removal
UV-MW	60	95	33.6
H_2O_2/UV-MW	60	95	25.7
Fe^{3+}/H_2O_2/UV-MV	60	95	30.8
US/NH_4NO_3/MeOH	15	50	92.1
Calcined	6000	550	100

Further investigation over these methodologies was not carried out since one of the aims of this work is to avoid surfactant degradation. The recovery and recycling of the surfactant in the synthesis of MCM-41 materials is discussed in the following section.

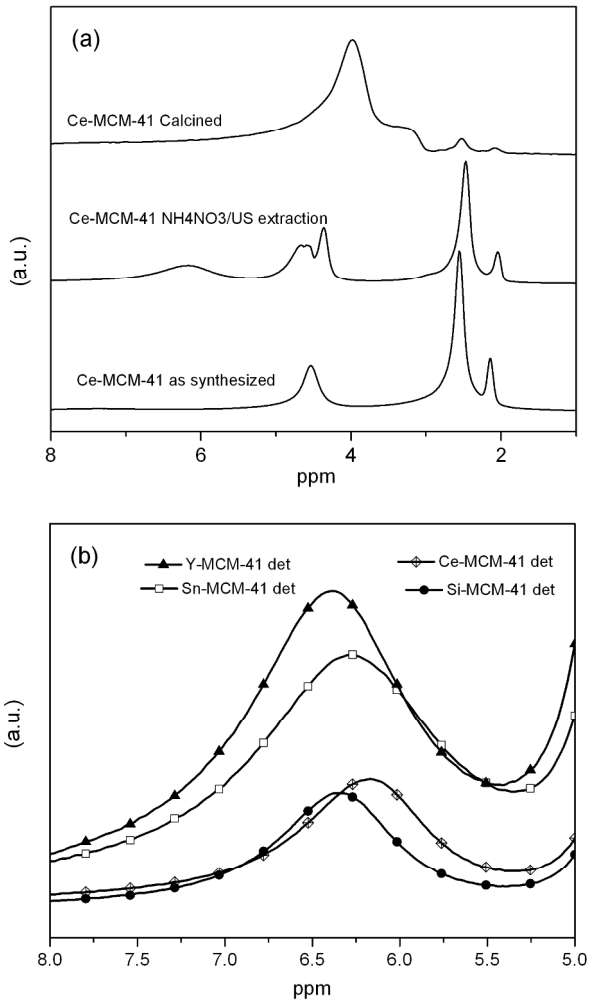

Figure 6. Ultrafast ^{1}H MAS NMR spectra of: a) the modified Ce-MCM-41 mesoporous material and b) M-MCM-41 surfactant removal by NH_4NO_3/US/MeOH extraction.

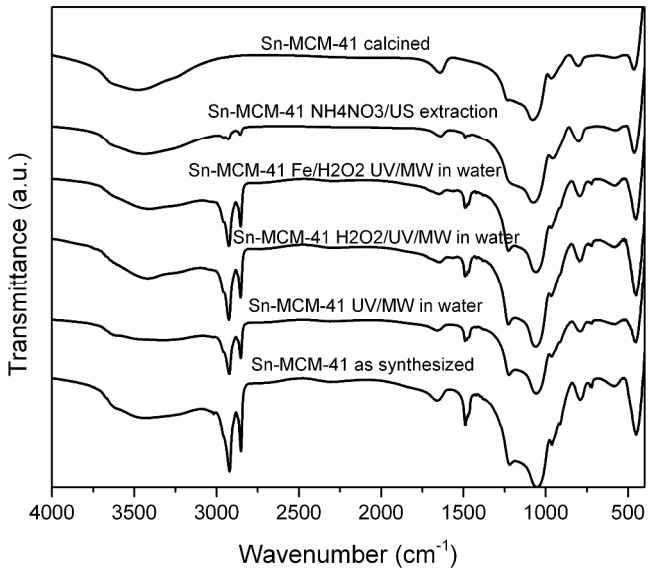

Figure 7. FTIR spectra for Sn-MCM-41 after different treatments applied to remove the surfactant through oxidative removal.

2.5 Recovery and re-use of CTAB: fast and convenient Si-MCM-41 synthesis approach.

Considering the reduction of time and energy demands, an innovative and eco-friendly synthesis process for the MCM-41 mesoporous materials was investigated as well. First, Si-MCM-41 was synthesized in a hydrothermal microwave assisted process. The hydrothermal time was reduced from 24 to 2 h using a coaxial applicator to introduce the microwave energy into the hydrothermal reactor. Since the hydrothermal crystallization time was significantly reduced, direct energy saving was also involved.

After the microwave hydrothermal synthesis, this material was submitted to the NH_4NO_3/US/MeOH surfactant extraction explored in section 2.2.

Finally, the CTAB was recovered and it was used to synthesize a new batch of Si-MCM-41 without the use of fresh surfactant. The FTIR spectra in Figure 8a shows that the quality of the surfactant recovered after the detemplation step is kept, indicating that the NH_4NO_3/US/MeOH surfactant extraction does not induce significant surfactant degradation. The MCM-41 obtained from recovered surfactant also exhibits high crystallinity and hexagonal structure (see Figure 8b). The SAXS patterns for the MCM-41 synthesized by conventional hydrothermal synthesis and microwave assisted hydrothermal synthesis (MW-HT) reveal that both materials have hexagonal crystalline structure, exhibiting the four main diffraction peaks.

Thus, the microwave assisted hydrothermal synthesis proves to be effective and time saving. High aggregation patterns with the typical worm-like morphology and particle size (around 0.5 μm) is shown in Figure 4d. The reuse of CTAB implies a saving of about 50% in raw material costs. Moreover, the distilled methanol can also be reused in a new extraction step. The CTAB/Methanol separation process does not require too much energy in comparison to the energy needed to achieve high temperature surfactant removal by calcination.

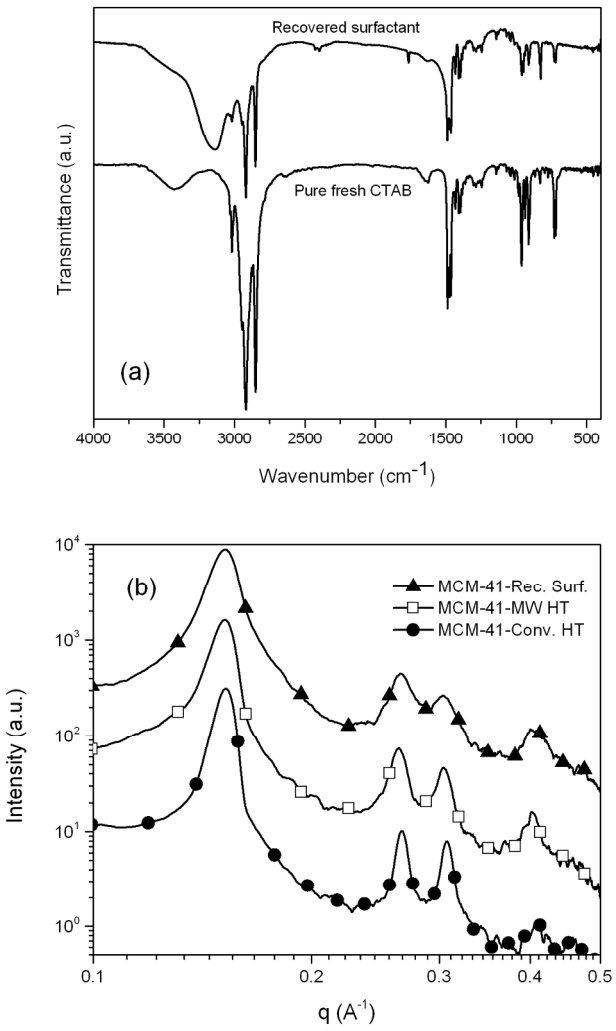

Figure 8. (a) FTIR spectra for the CTAB recovered (dried) compare to CTAB reagent and (b) SAXS for MCM-41-Rec.Surf. synthesized with recovered surfactant, Si-MCM-41-MW HT obtained by microwave assisted hydrothermal synthesis and MCM-41-Conv.HT synthesized by conventional hydrothermal synthesis.

3 Experimental

3.1 Materials

The following reagents were purchased from Sigma-Aldrich and used without further purification: Colloidal silica Ludox AS-40 (SiO_2, 40 wt. % suspension in water) and Tetraethyl orthosilicate ($Si(OC_2H_5)_4$, TEOS, 99.0% GC) were used as silicon source. Tetramethylammonium hydroxide ($N(CH_3)_4^+OH^-$, TMAOH 1 M in water) were used as co-surfactant in the synthesis of Sn-MCM-41 and Y-MCM-41. The templeate molecule was hexadecyltrimethylammonium bromide ($(C_{16}H_{33})N(CH_3)_3Br$, CTAB, 99%) for all material

synthesized. The metal salts: yttrium nitrate hexahydrate ($Y(NO_3)_3.6H_2O$, 99.8%), Cerium sulfate ($Ce(SO_4)_2$) and tin chloride pentahydrate ($SnCl_4.5H_2O$, 98%) were used as metal source for the modified MCM-41 synthesis. In the surfactant removal extraction, ammonium nitrate (NH_4NO_3, 99%) and methanol (CH_3OH, 99.9%) were used as salt cation donor and solvent respectively. Hydrogen peroxide (H_2O_2, solution 30% w/w in water, Carlo Erba) and iron nitrate nonahydrate ($Fe(NO_3)_3.9H_2O$, 98%) were used for the oxidative degradation experiments of the surfactant. Deionized Water obtained with a Milli-Q system (Millipore, Bedford, MA, USA) was used as solvent for all synthesis.

3.2 Synthesis of Si-MCM-41 , Sn-MCM-41, Y-MCM-41 and Ce-MCM-41 mesoporous materials by conventional hydrothermal process.

Two different samples of Sn-MCM-41 were prepared by direct incorporation of the metal into the synthesis gel following the methodology described by Gaydhankar and co-worker.[10] The synthesis procedure was as follows: 25 g of colloidal silica (Ludox AS-40) were slowly added to 49.93 g of TMAOH under magnetic stirring. To synthesize materials with molar ratios Si/Sn equal to 125 and 225, the right amount of $SnCl_4.5H_2O$ was dissolved in 5 ml of water and then added dropwise to the SiO_2-TMAOH dispersion and stirred for 1 h at 300 rpm. Then, 14.66 g of CTAB dissolved in 8.62 g of water and were slowly added to this solution and the mixture was stirred for 1 h at 600 rpm and transferred to a bath with ultrasound radiation (Ultrasonic Cleaner Branson 1510) where the formed gel remained under these conditions for 60 min. The final composition of the precursor gel was:

$$SiO_2 : 0.008\ SnO_2 : 0.24\ CTAB : 0.30\ TMAOH : 25\ H_2O$$

To prepare the Y-MCM-41 mesoporous material, the same methodology of Sn-MCM-41 was applied but the calculations were done to obtain 20 g of final product (dry and detemplated siliceous based powder). The final composition of the precursor gel was:

$$SiO_2 : 0.004\ Y_2O_3 : 0.24\ CTAB : 0.30\ TMAOH : 25\ H_2O$$

For Ce-MCM-41 materials, the molar ratios synthesized were Si/Ce equal 50 and 225. Both samples were prepared according to the methodology reported elsewhere.[11] The synthesis was carried out when 2.85 g of CTAB were dissolved in 50 ml of deionized water and 50.75 ml of NH_4OH, 20%. After having stirred for 0.5 h, a second solution containing the required amount of $Ce(NO_3)_36H_2O$ diluted in 12.5 ml of deionized water was added. Then, 5.7 ml of tetraethylorthosilicate were added dropwise at 40 °C. Homogeneity was increased by transferring the gel to a bath with ultrasound radiation (Ultrasonic Cleaner Branson 1510) for 2.5 h and then aged at 500 rpm for another 4 h. The final composition of the precursor gel was (where $x = 50^{-1}$ or 225^{-1}):

$$SiO_2 : x\ CeO_2 : 0.30\ CTAB : 10\ NH_4OH : 212\ H_2O$$

For comparative studies Si-MCM-41 was synthesized following the same procedure of Ce-MCM-41 but without the addition of metal salt to the synthesis gel. The final composition was (where $x = 125^{-1}$ or 225^{-1}):

$$SiO_2 : x\ SnO_2 : 0.24\ CTAB : 0.30\ TMAOH : 25\ H_2O$$

The different synthesis gel precursors were hydrothermally treated in a Teflon-lined stainless steel reactor at 110 °C for 72 h for Sn- and Y-MCM-41 materials and 100 °C for 24 h in the cases of Ce- and Si-MCM-41. The process was carried out at autogenous pressure under static conditions. Finally, the precipitate was separated by centrifugation, washed with deionized water and dried at 80 °C overnight.

3.3 Surfactant removal procedure

3.3.1 Ultrasound-assisted ion exchange extraction in methanol (NH_4NO_3/US/MeOH surfactant extraction)

The surfactant removal by low temperature NH_4NO_3/US/MeOH surfactant extraction was investigated using low frequency ultrasound energy. A typical experiment was performed using a sonicator Vibra cell sonics (VCX 750) with a frequency of 20 KHz and a tip diameter of 13 mm. To explore the effect on the metal modified structures, a response surface methodology was used to find the best conditions for the surfactant removal of Y-MCM-41 and these conditions were applied to the remaining structures. Y-MCM-41 structure was chosen due to its high Si/Y molar ratio. A three factors Box-Behnken design was chosen with the following factors: x_1 = the salt cation donor concentration (NH_4NO_3), x_2 = the ultrasound amplitude and x_3 = the contact time. Table 6 shows the boundary values for the factors involved in the NH_4NO_3/US/MeOH surfactant extraction.

Table 6. Box-Behnken design boundary values for the ultrasound assisted ion-exchange surfactant removal from metal modified MCM-41

Parameter	Boundary Values		
	-1	0	+1
x_1	0	25	50
x_2	22	40	60
x_3	5	10	15

[A] [x1] = mM, [x2] = %, and [x3] = min

A typical run was carried out as follow: 0.5 g of the Y-MCM-41 material was loaded in a glass beaker contained the corresponding quantity of NH_4NO_3 dissolved in 80 ml of methanol. The baker was kept under ultrasound irradiation for the appropriate time, while the mixture was magnetically stirred at 300 rpm under adiabatic temperature. The product was recovered by centrifugation, washed with cold methanol and dried at 80 °C overnight.

3.3.2 Oxidative degradation: UV/MW, H_2O_2/UV/MW and Fe^{3+}/H_2O_2/UV/MW aqueous systems using a photochemical reactor

Alternative studies to the solvent extraction were done using the Sn-MCM-41 material as comparative. For these experiments a photochemical reactor was used. In this reactor, ultraviolet and microwave energy are simultaneously applied to a liquid sample and it resulted in a very efficient and fast degradation of the organic molecules in diluted hydrogen peroxide aqueous solutions.[32] Three different approaches were investigated: 1) electromagnetic energy (UV/MW) irradiation, 2) diluted oxidative agent (400 ppm of H_2O_2)+UV/MW and 3) an iron salt concentration of 20 ppm and 400 ppm of H_2O_2 (the photo-Fenton system) + UV/MW. The experiments were carried out loading 0.5 g of Sn-MCM-41 in 90 ml of milliQ into the photoreactor. Then a microwave power of 50 W at 2.45 GHz was applied and the temperature increased to the boiling point. The dispersion was kept under reflux for 60 min after that the electromagnetic energy was switch off and the powder was separated by centrifugation, washed with water and dried at 80 °C overnight.

3.3.4 Calcination

The conventional calcination process was also used to remove the surfactant from the as-synthesized samples at high temperature. The dried powders were calcined using a 1 °C/min temperature heating rate to 550 °C and then keeping it for 6 h under air atmosphere conditions.

3.4 Recovery and re-use of CTAB in a microwave hydrothermal synthesis of Si-MCM-41

The CTAB/Methanol solution obtained after the surfactant removal process described in section 3.3.1 was distilled until a minimal quantity of methanol remained in the flask bottom at 70 °C. The distilled methanol was recovered and saved for its re-use in future extractions. The remaining solution was evaporated at 40 °C until a white dry precipitated was obtained. The white powder was FTIR analysed and it showed identical adsorption bands than the CTAB reagent from Sigma-Aldrich (see Figure 8a). A weighed quantity of the recovered CTAB was used without any other treatment to prepare a new Si-MCM-41 synthesis gel following the methodology describe in section 2.2. The hydrothermal process was microwave assisted using a high pressure microwave reactor with a microwave coaxial applicator describes in a previous work.[33] After the aging process for 6 hrs at 50 °C the resultant gel was transferred to the Teflon vessel and loaded in the high pressure reactor. The microwave power was applied and the synthesis gel was kept under MW irradiation for 2 hrs under autogenous pressure and static conditions at 100 °C. The recovery of the Si-MCM-41, CTAB and methanol was once again carried out as mentioned above.

3.5 Characterization

3.5.1 Small Angle X-ray Scattering (SAXS)

SAXS measurements for the as-synthesized, calcined and NH_4NO_3/US/MeOH surfactant extraction treated materials were carried out with a HECUS S3-MICRO camera (Kratky-type) equipped with a position-sensitive detector (OED 50M) containing 1024 channels of width 54 μm. Cu Kα radiation of wavelength λ = 1.542 Å was provided by an ultra-brilliant point micro-focus X-ray source (GENIX-Fox 3D, Xenocs, Grenoble), operating at a maximum power of 50 W (50 kV and 1 mA). The sample-to-detector distance was 281 mm. The volume between the sample and the detector was kept under vacuum during the measurements to minimize scattering from the air. The Kratky camera was calibrated in the small angle region using silver behenate (d = 58.34 Å).[34] Scattering curves were obtained in the q-range between 0.01 and 0.54 $Å^{-1}$, assuming that q is the scattering vector, $q = 4\pi/\lambda \sin\theta$, and 2θ the scattering angle. Powder samples were placed into a 1 mm demountable cell having Nalophan foils as windows. The temperature was set to 25 °C and was controlled by a Peltier element, with an accuracy of 0.1 °C. All scattering curves were corrected for the empty cell contribution considering the relative transmission factor. The hexagonal unit cell is given as $a_0 = 2d_{100}/\sqrt{3}$

3.5.2 FTIR Spectroscopy

FTIR spectroscopy was used to determine the relative percent removal of the surfactant from the mesoporous structures. Quantitative analysis were done by measuring the area under the absorption peaks assigned to the vibrations of surfactant molecule, pelleting the samples with KBr. Spectra were recorded in the range 4000 - 400 cm^{-1} using a Spectrum 100 FTIR spectrophotometer (PerkinElmer Inc., USA). The FTIR spectra were baseline-corrected and normalized at 1095 cm^{-1}. The percentage of surfactant removed (% removal) was calculated considering the total area of the synthesized M-MCM-41 material as 100%.

3.5.3 N_2 physisorption

Nitrogen adsorption/desorption isotherms were recorded at -196 °C on a Micromeritics ASAP 2010 instrument. The specific surface area (S_{BET}) was calculated using BET method[35] and the external surface area (ESA) was calculated with the t-plot method.[36]

3.5.4 Thermogravimetric analysis (TGA)

As comparative proof of template removal thermal gravimetric analysis were carried out using a TA Instruments Thermobalance model Q5000IR. Measurements were performed at a rate of 10 °C min^{-1}, from 40 °C to 600 °C under air flow (25 mL min^{-1}). The amount of sample in each TGA measurement varied between 2 and 4 mg.

3.5.5 Scanning Electron Microscopy (SEM)

The morphology and particle size were analyzed using a SIGMA field emission scanning microscope (Carl Zeiss Microscopy GmbH, Germany) directly on uncoated samples. The reported images were acquired using the In-Lens Secondary Electron detector. The metal loaded into the

framework was determined using Energy-dispersive X-ray spectroscopy (EDS) that was performed by a 10 mm^2 silicon drift detector (X-Act) coupled with the SEM microscope operated by the INCA software (Oxford Instruments). In this second case, the operative voltage of the electron source was about 20 kV and the working distance 8.5 mm to maximize the X-ray photon counts.

3.5.6 1H MAS, 29Si HPDEC MAS NMR

Solid state NMR spectroscopy studies were recorded on a Bruker Avance II 300 spectrometer.

^{1}H MAS NMR measurements were performed at a resonance frecuency of 300 MHz. 1,3 mm ZrO_2 rotor was spun at 50 KHz. 4 µs Flip angle was used (90°), the recycling time was 3 s using a VF CPMAS H-X BB 1.3 mm probe.

^{29}Si HPDEC MAS NMR were acquired using a CPMAS H-X BB 4 mm probe at a resonance frequency of 59 MHz, the recycling time was 10 s. 4 µs Flip angle was used (90°) with an acquisition time of 10 ms.

4 Conclusions

A novel methodology incorporating ultrasound irradiation in an ion-exchange approach was successfully applied to remove the surfactant from various metal modified mesoporous materials. The nature and amount of metal present in the MCM-41 structure proved to have a significant effect on the quantity of surfactant removed, ranging from 90% and up to 99% after 15 min of adiabatic treatment.

This methodology does not cause considerable textural nor structural differences in the final materials and reduces the thermal shrinkage produced by the conventional calcination surfactant degradation. The hexagonal structure was kept and high areas were obtained after the extraction treatment. Moreover, the surface silanol loss produced by high temperature surfactant removal can be lessened and more silanolic sites are preserved, making the design of specific materials very feasible, depending on the hydrophobic and hydrophilic characteristics desired. These materials could be potentially used in different applications, like catalytic supports or as matrix for absorption purposes.

It was proved that the removed surfactant can be recycled in the synthesis of new mesoporous material, with clear advantages in terms of cost and CO_2 emission. The reduction of the environmental impact can also be reached through the use of innovative methodologies, such as the microwave-assisted synthesis.

We have shown that a synthesis performed with recycled surfactant and microwave-irradiation has structural characteristics indistinguishable from those of the mesoporous material obtained with conventional synthesis.

The existent synergy between the methodologies used (US and MW irradiation) to assist the chemistry involved in the synthesis process can lead to promising scale up projections for the industrial production and application of these modified materials, without any technological barrier.

Acknowledgements

The authors wish to acknowledge the National Council of Science and Technology (CONACYT México, project CB-2010-158193) and the Consorzio per lo Sviluppo dei Sistemi a Grande Interfase (CSGI), for providing financial support.

The authors would like to thank C. Lanza and F. Pardini (INO-CNR). The authors also would like to thank Marco Vera (UAM-I) for their valuable technical support.

Notes and references

[a]*Chemical Engineering Department, University of Guanajuato, Noria Alta s/n 36050, Guanajuato, Gto. (Mexico).*
[b]*National Research Council of Italy (C.N.R.), Istituto di Chimica dei Composti Organo Metallici (ICCOM) - UOS Pisa, Via G. Moruzzi 1, 56124 Pisa (Italy).*
[c]*Department of Chemistry and Industrial Chemistry, University of Pisa, Via Risorgimento 35 - 56127 Pisa (Italy).*
[d]*National Research Council of Italy (C.N.R.), Istituto Nazionale di Ottica, (INO) – UOS Pisa, Via G. Moruzzi 1, 56124 Pisa (Italy).*
[e]*Department of Chemistry "Ugo Schiff" and CSGI, University of Florence, Via della Lastruccia 3 − 50019 Sesto Fiorentino, Florence (Italy).*
**Corresponding author. E-mail: carlo.ferrari@ino.it; Tel: +39-050-315-2245; Fax: +39-050-315-2247.*

1 R. M. Martín-Aranda and J. Cejka, *Top Catal*, 2010, **53**, 141-153.
2 S. Bhattacharyya, G. Lelong and M. L. Saboungi, *J Exp. Nanosci.*, 2006, **3**, 375-395.
3 B. Naik and N. N. Ghosh, *Rec. Pat. Nanotech.*, 2009, **3**, 213-224.
4 C. T. Kresge, M. E. Leonowicz, W. J. Roth, J. C. Vartuli and J. S. Beck, *Nature*, 1992, **359**, 710-712.
5 A. Corma, A. Matinez, V. Martinezsoria and J.B. Monton, *J. Catal*, 1995, **153**, 25-31.
6 M. Popova, Á. Szegedi, Z. Cherkezova-Zheleva, I. Mitov, N. Kostova and T. Tsoncheva, *J. Hazard. Mater.*, 2009, **168**, 226-232.
7 J. Felipe Díaz and K. J. Balkus Jr, *J. Mol. Catal. B - Enzym.*, 1996, **2**, 115-126.
8 H. P. Yiu, P. A. Wright and N. P. Botting, *J. Mol. Catal. B - Enzym.*, 2001, **15**, 81-92.
9 A. Corma, *Chem. Rev.,* 1997, **97**, 2373-2419.
10 T.R. Gaydhankar, P.N. Joshi, P. Kalita and R. Kumar, *J. Mol. Catal. A - Chem.*, 2007, **265**, 306-315.
11 J.C. Guevara, J.A. Wang, L.F. Chen, M.A. Valenzuela, P. Salas, A. García-Ruiz, J.A. Toledo, M.A. Cortes-Jácome, C. Angeles-Chavez and O. Novaro, *Int. J. Hydrogen. Energy*, 2010, **35**, 3509-3521.
12 G.D. Mihai, V. Meynen, E. Beyers, M. Mertens, N. Bilba, P. Cool and E. F. Vansant, *J. Porous Mater*, 2009, **16**, 109-118.
13 J. Patarin, *Angew. Chem. Int. Ed.*, 2004, **43**, 3878-3880.
14 J. He, X. Yang, D.G. Evans and X. Duan, *Mater. Chem. Phys.*, 2002, **77**, 270-275.
15 Y. Liu, Y. Pan, Z. Wang, P. Kuai and C. Liu, *Catal. Commun.*, 2010, **11**, 551-554.
16 A. Marcilla, M. Beltran, A. Gómez-Siurana, I. Martinez and D. Berenguer, *Chem. Eng. Res. Des.*, 2011, **89**, 2330-2343.

17 B. Tian, X. Liu, C. Yu, F. Gao, Q. Luo, S. Xie, B. Tu and D. Zhao, *Chem. Commun.*, 2002,1186-1187.
18 L. López Pérez, M. J. Ortiz-Iniesta, Z. Zhang, I. Agirrezabal-Telleria, M. Santes, H. J. Heeres and I. Melián-Cabrera, *J. Mater. Chem. A*, 2013, **1**, 4747-4753.
19 S. Hitz and R. Prins, *J. Catal.*, 1997, **168**, 194-206.
20 N. Lang and A. Tuel, *Chem. Mater.*, 2004, **16**, 1961-1966.
21 S. Jabariyan and M. A. Zanjanchi, *Ultrason. Sonochem.*, 2013, **19**, 1087-1093.
22 Z. Huang, H. Miao, J. Li, J. Wei, S. Kawi and M.W. Lai, *Sep. Purif. Technol.*, 2013, **118**, 170-178.
23 J. S. Beck, J. C. Vartuli, W. J. Roth, M. E. Leonowicz, C. T. Kresge, K. D. Schmitt, C. T. W. Chu, D. H. Olson and E. W. Sheppard, *J. Am. Chem. Soc.*, 1992, **114** (27), 10834-10843.
24 J. M. Kim, J. H. Kwak, S. Jun and R. Ryoo, *J. Phys. Chem.,* 1995, **99**, 16742-16747.
25 Z. Zhang, J. Yin, H.J. Heeres and I. Melián-Cabrera, *Micropor. Mesopor. Mat.*, 2013, **176**, 103-111.
26 S. P. Brown, Solid State Nuclear Magnetic Resonance, 2012, **41**, 1-27.
27 M. Müller, G. Harvey, R. Prins, Microporous and Mesoporous Materials 2000, **34**, 281-290.
28 D. W. Sindorf , G. E. Maciel. Am. Chem. Soc., 1983, **105** (6), pp 1487–1493.
29 J. Trébosc, J. W. Wiench, S. Huh, V. S.-Y. Lin, M. Pruski, J. Am. Chem. Soc., 2005, 127(9), 3057-3068.
30 B. Grünberg, T. Emmler, E. Gedat, I. Shenderovich, G. H. Findenegg, H.H. Limbach, G. Buntkowsky, Chem. Eur. J. 2004, 10, 5689-5696.
31 J. Walia, J. Crone, J. Liang, M. Niknam, C. Lemaire, R. T. Thompson, H. Peemoeller, Solid State Nuclear Magnetic Resonance, 2013, 49–50, 26–32.
32 C. Ferrari, I. Longo, E. Tombari and E. Bramanti, *J. Photoch. Photobio. A: Chem.*, 2009, **204**, 115-121.
33 J. González-Rivera, I. R. Galindo-Esquivel, M. Onor, E. Bramanti, I. Longo and C. Ferrari, *Green Chem*, 2013, DOI:10.1039/C3GC42207K.
34 T. N. Blanton, M. Rajeswaran, P. W. Stephens, D. R. Whitcomb, S. T. Misture and J. A. Kaduk, *Powder Diffraction*, 2011, **26**, 313-320.
35 S., Brunauer, P.H., Emmett and E. Teller, *J. Am. Chem. Soc.*, 1938, **60**, 309.
36 B. C. Lippens, B. G. Linsen and J. H. de Boer, *J. Catal.*, 1964, **3**, 32.